Electrostatic Disturbance Forces on a Three-Axis Drag-Free Sensor

A. Vijayaraghavan* and D. Sonnabend†
Jet Propulsion Laboratory, California Institute of Technology, Pasadena, California
and
T. Hagstrom‡
California Institute of Technology, Pasadena, California

The electrostatic analysis of a multi-capacitance three-axis drag-free sensor is presented herein. The instrument consists of a proof-mass (a dense metallic ball) floating freely inside a spherical cavity enclosed by the sensor plates and the shield. The electrostatic disturbances on the proof-mass depend on both the amount of charge and the proof-mass plate geometry. Since the ball and the cavity are not necessarily concentric, the problem in three-dimensional potential theory for electrostatics is solved by the method of boundary perturbations and specifically in terms of spherical harmonics. The capacitance outputs of the instrument and the electrostatic forces acting on the system are derived as nonlinear functions of the ball position, ball charge, and the sensor plate potentials. The instrument sensitivity and cross-coupling effects are discussed. The analysis may be useful for electrostatic gyros and suspensions also.

Nomenclature

a	= proof-mass radius
$A_n^{(i)m}$	= expansion coefficient, as in Eq. (37), of the eigenfunction of order m, degree n, for the potential $U^{(i)}$
A_n	= $A_n^{(0)0}$; see Eq. (35)
b	= cavity radius
C_{ij}	= mutual capacitance coefficient
C_{ii}	= self-capacitance coefficient
d	= proof-mass displacement (Fig. 1)
$D_n^{(1)m}$	= coefficients in Eqs. (40) and (42)
$D_n^{(2)m}$	= coefficients in Eqs. (49) and (50)
$E_n^{(2)m}, F_n^{(2)m}$	= coefficients in Eqs. (47) and (48)
E_i	= stored electrical energy in the ith conductor
F	= vector force
$I(m,n)$	= integral in Eq. (66)
$P_n(\mu)$	= Legendre polynomial of degree n of the argument μ; $-1 \le \mu \le +1$
$P_n^m(\mu)$	= associated Legendre function of the first kind, order m, degree n
Q_i	= charge on the ith conductor
r	= spherical radius
$R_n^{(i)}$	= radial function in Eqs. (34) and (38)
S_1	= proof-mass surface
S_2	= cavity wall surface
S_p	= sensor plate 1 surface
$U^{(i)}$	= ith order perturbation potential
V_i	= potential of the ith conductor
x,y,z	= proof-mass center coordinates normalized to b, see Eq. (57)
X,Y,Z	= Cartesian coordinate axes
α	= a/b
β_k	= $(1+\alpha^k)/(1-\alpha^k)$
γ	= angle shown in Fig. 1
ϵ_0	= free-space permittivity
η	= $\cos\theta^*$
θ	= spherical polar angle
θ^*	= polar angle of the sensor plate boundary as in Fig. 1
θ_0	= polar angle of proof-mass center (Fig. 1)
ϕ	= azimuthal angle
ϕ_0	= angle shown in Fig. 1
ω	= frequency, rad/s
Δ	= incremental operator
∇	= gradient operator
∇^2	= Laplacian operator
$\partial/\partial r$	= partial derivative with respect to r

Presented as Paper 82-0046 at the AIAA 20th Aerospace Sciences Meeting, Orlando, Fla., Jan. 11-14, 1982; submitted Jan. 29, 1982; revision received June 20, 1983.

*Member of the Technical Staff.
†Member of the Technical Staff. Member AIAA.
‡Graduate Student in Applied Mathematics.

Introduction

MISSION design studies on STARPROBE,[1] GRAVSAT,[2] and TOPEX[3] have indicated the need to develop a highly accurate drag-free sensor capable of measuring low-level acceleration correct to within 10^{-11} m/s^2. For instance, such high sensitivity is essential[4] to carry out scientific experiments in solar structure and gravitational theory during the STARPROBE mission in the late 80's.

Description of the Sensor

The basic concept of a multiple-capacitance drag-free sensor is given in detail in Ref. 5. Such an instrument has been flown successfully in Earth orbit in the TRIAD[6] satellite. The sensor apparatus, schematically shown in Figs. 1 and 2, consists of a proof-mass (a metallic sphere) suspended freely in vacuum inside a spherical shield attached to the spacecraft. Between the shield and the ball there are six thin spherical caps or plates located at the ends of three mutually perpendicular axes; the plates are isolated from the shield and the ball and are kept at desired potentials. From capacitance measurements on the sensor instrument, in addition to data on the instantaneous position and velocity of the ball relative to the cavity, more precise information can be obtained on the gravitational trajectory. The device is similar to other electrostatically supported, spherical accelerometers such as the CACTUS[7,8] developed by ONERA and Honeywell ESA.[9]

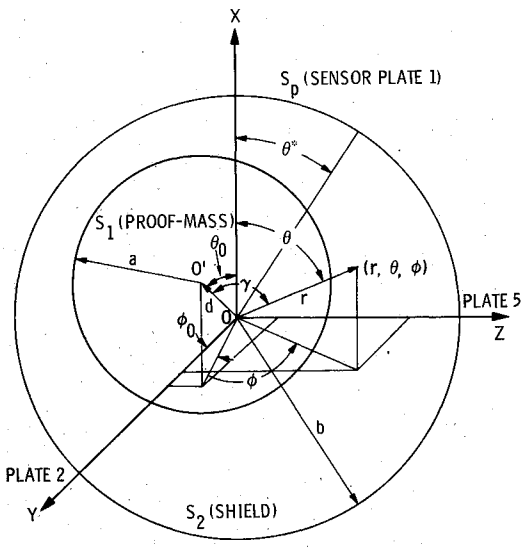

Fig. 1 Schematic diagram of the drag-free sensor. Sensor plates 3, 4, and 6 are placed diametrically opposite to plates 1, 2, and 5, respectively.

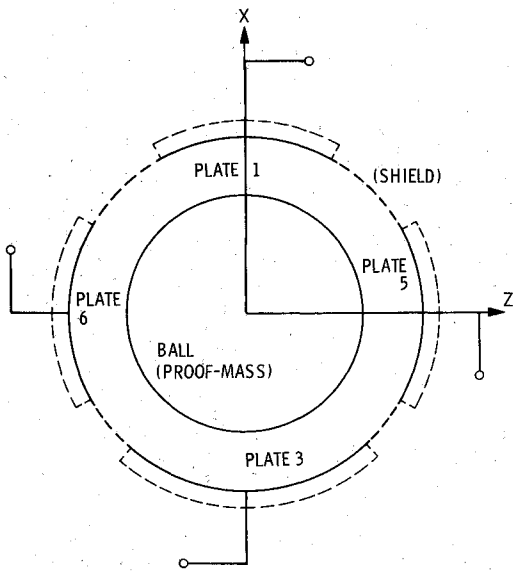

Fig. 2 Cross-sectional view of the drag-free sensor with the proof-mass in its nominal position concentric with the cavity center.

Although solar pressure and forces due to meteorites and particles impingement do not act on the proof-mass, it is still subject to disturbances such as the self gravity of the spacecraft and the electrostatic forces due to charges accumulated on isolated parts of the spacecraft as it travels by Jupiter and the sun.

Analysis

The electrostatic force acting on the system is derived from the principle of virtual work.[10] The force depends not only on the potentials and charge on the conductors, but also on the self- and mutual-capacitance coefficients (of the sensor elements) and their spatial derivatives. In turn, the capacitance values and their gradients are obtained by solving appropriate problems in potential theory.

Exworthy[9] has given an approximate solution for the capacitance of a sphere in the vicinity of a single spherical cap by integrating the local incremental capacitance for infinite parallel plate condensers. His results are satisfactory if the sphere and plate are "sufficiently" well separated. With a better approximation to the geometry, Sonnabend[5] has obtained results more closely in agreement with the logarithmic nature of the capacitance when the ball and plate walls are close to each other; however, it was necessary to restrict the ball to travel along the symmetry axis of the spherical cap.

Although such approximation may be formally extended to the three-axis instrument under consideration, in the analysis it would still be necessary to ignore 1) the effects of the mutual capacitance of the various plates, 2) the edge effects, and 3) the presence of a grounded shield. It is in this context that the actual sensor system is considered for three-dimensional analysis in the present work.

Electrostatic Forces

The drag-free sensor consists of a set of eight conductors, labeled 0 for the proof-mass (ball), 1-6 for the plates, and 7 for the outer shield. Let V_i and Q_i denote the potential and charge, respectively, on the ith conductor. Then the electrostatic energy stored in it is given by[11]

$$E_i = \tfrac{1}{2} V_i Q_i \tag{1}$$

The charge is related to the potentials as in[12]:

$$Q_i = \sum_{j=0}^{6} C_{ij} V_j \tag{2}$$

where C_{ij} is the mutual capacitance between the ith and jth conductors and C_{ii} denotes the self capacitance of the ith conductor. In general, C_{ij}'s are functions only of the system geometry and hence they all will change when the ball moves.

To find the electrostatic force on the system consider an infinitesimal virtual displacement Δr of the ball. Assuming the plates are connected to external "power" supply at constant potentials, the ball displacement will cause changes only in the plate charges ΔQ_i (i=1-6) and in the ball potential, ΔV_0. Thus, from Eq. (1), the total electrostatic energy in the system would change by an amount,

$$\Delta E = \frac{1}{2} Q_0 \Delta V_0 + \frac{1}{2} \sum_{i=1}^{6} V_i \Delta Q_i \tag{3}$$

The charge ΔQ_i must be due to a current I_i from the potential source, V_i; so, the external sources together must provide an amount of energy,

$$\Delta E_p = \sum_{i=1}^{6} V_i \int_0^\infty I_i \mathrm{d}t = \sum_{i=1}^{6} V_i \Delta Q_i \tag{4}$$

From the law of conservation of energy, the virtual work done on the ball must be equal to the energy supplied less the change in the total electrostatic energy:

$$\boldsymbol{F} \cdot \Delta \boldsymbol{r} = \Delta E_p - \Delta E = \frac{1}{2} \sum_{i=1}^{6} V_i \Delta Q_i - \frac{1}{2} Q_0 \Delta V_0 \tag{5}$$

From Eq. (2), the various changes are related by,

$$\Delta Q_i = C_{i0} \Delta V_0 + \sum_{j=0}^{6} V_j \Delta C_{ij} \tag{6}$$

Also, the proof-mass potential V_0 can be solved in terms of its charge Q_0 from Eq. (2) as in

$$V_0 = \left(\frac{1}{C_{00}}\right)\left\{Q_0 - \sum_{j=1}^{6} C_{0j} V_j\right\} \tag{7}$$

Deriving the incremental quantity ΔV_0 from Eq. (7) and substituting it into Eqs. (5) and (6),

$$F\cdot\Delta r=\frac{1}{2}\sum_{i=0}^{6}\sum_{j=0}^{6}V_iV_j\Delta C_{ij} \tag{8}$$

Finally, since the C_{ij}'s depend only on geometry,

$$\Delta C_{ij}=\nabla C_{ij}\cdot\Delta r \tag{9}$$

and as Δr is arbitrary,

$$F=\frac{1}{2}\sum_{i=0}^{6}\sum_{j=0}^{6}V_iV_j\nabla C_{ij} \tag{10}$$

The unknown potential V_0 is obtained from Eq. (7) if the ball charge Q_0 is known. Although V_0 is linear in Q_0 and the V_j's, from Eq. (10) it is seen that F is a quadratic function in Q_0 and the sensor plate potentials.

Capacitance Coefficients, C_{ij}

The mutual capacitance coefficient C_{ij} is defined[13] as the charge induced on the jth conductor, when the ith conductor is maintained at unit potential and all other conductors in the system (except the ith) are grounded. In fact, with these prescribed potentials on the conductors as boundary conditions, if U denotes the potential distribution in space, it follows from Gauss' law[14] that

$$C_{ij}=-\epsilon_0\int_{\Sigma_j}\nabla U\cdot n\,ds \tag{11}$$

where Σ_j denotes a surface that encloses only the jth conductor and n denotes a unit normal at each point on Σ_j, positive outward. When $j=i$, the surface integral in Eq. (11) gives the self-induced charge or self-capacitance coefficient.

The potential distribution U, in turn, is obtained by solving Laplace's equation[15] with appropriate boundary conditions. With the relevant subscripts (i,j) ranging from 0 through 6, seemingly many cases need to be considered. However, the superposition principle for potential distribution, the reciprocity theorem for capacitance coefficients ($C_{ij}=C_{ji}$) and coordinate transformations help to narrow down the problem to one most typical case.

Boundary-Value Problem for the Potential

In Fig. 1 is shown the most general configuration of the drag-free sensor, for which the potential distribution must be obtained under appropriate boundary conditions.

S_1 represents the proof-mass of radius a with its center at O′ floating freely inside the cavity attached to the spacecraft. The cavity center is coincident with the origin O of the reference Cartesian coordinate system X-Y-Z. The six sensor (or potential) plates, which are thin spherical metallic caps, lie on the cavity wall surface S_2 of radius b. The symmetry axis of plate 1 is collinear with the X axis, with the plate intersecting the positive X axis. Plate 2 lies on the surface S_2, symmetrically located about the positive Y axis. Plates 3 and 4 are placed diametrically opposite plates 1 and 2, respectively, intersecting the $-X$ and $-Y$ axes appropriately. Plates 5 and 6 are also on surface S_2 with their symmetry axes collinear with the Z axis and the plates intersecting the Z axis on the positive and negative sides, respectively. Each sensor plate subtends a cone of semivertical angle θ^* at the center, O. The spherical grounding shield has a radius slightly larger than b; however, for analysis, it will be assumed that the *grounding shield lies on the surface* S_2. exclusive of the sensor plates.

Spherical Coordinate System

The line of centers O-O′ is in some arbitrary direction, not collinear with any coordinate axis X, Y, or Z of the Cartesian system. Let the distance O-O′ $=d$. The problem will be solved in a spherical coordinate system with its origin at O, the cavity center and the polar axis coincident with the X axis with the same positive direction. The spherical polar angle θ is measured from the X axis or the polar axis. The azimuthal angle ϕ is measured anticlockwise on the horizontal Y-Z plane from a reference line where the vertial plane containing the line of centers OO′ and the X axis intersects the Y-Z plane.

Statement of the Problem

Suppose the capacitance coefficients C_{10} $C_{11},\ldots,C_{16}$ are to be evaluated. It is necessary to solve Laplace's equation for the potential distribution U, when plate 1 is held at unit potential and the other five sensor plates, the shield (the surface S_2 exclusive of plate 1), and the proof-mass (with its surface S_1) are at zero or ground potential. In mathematical terms,

$$\nabla^2U=0 \text{ between } S_1 \text{ and } S_2 \tag{12}$$

$$U(S_p)=1\ (S_p:\ r=b;\ 0\le\theta\le\theta^*;\ 0\le\phi\le2\pi) \tag{13}$$

$$U(S_2-S_p)=0\quad(r=b;\ \theta^*<\theta\le\pi;\ 0\le\phi\le2\pi) \tag{14}$$

$$U(S_1)=0 \tag{15}$$

Perturbation Equations[16]

The proof-mass center is located at $(d,\theta_0,0)$ in the spherical coordinate system described. However, for sufficiently small values of d, the proof-mass surface S_1 can be considered a small deviation from the spherical surface, $r=a$. For every set of values (θ,ϕ), the radius vector $r(S_1;\theta,\phi)$ is related to (a,θ,ϕ) as in

$$a^2=r^2(S_1;\theta,\phi)-2d\,r(S_1;\theta,\phi)\cos\gamma+d^2 \tag{16}$$

where

$$\cos\gamma=\cos\theta\cos\theta_0+\sin\theta\sin\theta_0\cos\phi \tag{17}$$

Actually, γ is the angle between the line of centers O-O′ and the radius vector (r,θ,ϕ) as shown in Fig. 1. Solving Eq. (16) as a quadratic in $r(S_1;\theta,\phi)$, it is easily seen that,

$$r(S_1;\theta,\phi)=a\left\{1+\left(\frac{d}{a}\right)\cos\gamma-\frac{1}{2}\left(\frac{d}{a}\right)^2\sin^2\gamma+0\left(\frac{d}{a}\right)^3\right\} \tag{18}$$

Let the potential U be expanded in a perturbation power series, such as

$$u=U^{(0)}+dU^{(1)}+d^2U^{(2)}+\cdots \tag{19}$$

Consistent with Eqs. (12-15),

$$\nabla^2U^{(i)}=0 \tag{20}$$

$$U^{(0)}(S_p)=1;\ U^{(0)}(S_2-S_p)=0 \tag{21}$$

$$U^{(i)}(S_2)=0\ \ i=1,2,\ldots \tag{22}$$

The potential on the boundary S_1 can be written as follows:

$$U(S_1)=U(a,\theta,\phi)+\frac{\partial U}{\partial r}(a,\theta,\phi)\{r(S_1,\theta,\phi)-a\}+\frac{1}{2}\frac{\partial^2U}{\partial r^2}(a,\theta,\phi)\{r(S_1,\theta,\phi)-a\}^2+\ldots \tag{23}$$

From Eqs. (19) and (23), the boundary condition in Eq. (15) that the potential U be zero on the surface S_1 of the proof-

mass can be satisfied uniformly in the displacement d, provided,

$$U^{(0)}(a,\theta,\phi)=0 \tag{24}$$

$$U^{(1)}(a,\theta,\phi)=-\frac{\partial U^{(0)}}{\partial r}(a,\theta,\phi)\cos\gamma \tag{25}$$

and

$$U^{(2)}(a,\theta,\phi)=-\frac{\partial U^{(1)}}{\partial r}(a,\theta,\phi)\cos\gamma + \frac{\partial U^{(0)}}{\partial r}(a,\theta,\phi)\frac{\sin^2\gamma}{2a}-\frac{\partial^2 U^{(0)}}{\partial r^2}(a,\theta,\phi)\frac{\cos^2\gamma}{2} \tag{26}$$

Equations (20-22) together with Eqs. (24-26) completely define the potentials $U^{(0)}$, $U^{(1)}$, and $U^{(2)}$ with their boundary conditions prescribed on the surfaces S_1 and S_2 and satisfying Laplace's equation in the space between S_1 and S_2.

The perturbation scheme must be carried at least to the second order so that the resulting capacitance coefficients, when differentiated once, would still reflect first-order changes due to proof-mass displacement in the electrostatic force evaluated from Eq. (10). Also, it is a well-known result from the problem of two nested spheres[17] that the first nonzero correction term to the proof-mass self-capacitance is proportional to d^2.

Solutions for the Perturbation Potentials

The solutions for the potentials are obtained in terms of spherical harmonics.[18] In particular, the angular distribution in θ is expressed in terms of the associated Legendre functions of the first kind, $P_n^m(\cos\theta)$ of order m and degree n, or the Legendre polynomials $P_n(\cos\theta)$ in the axisymmetric case. Since Legendre functions of the second kind are unbounded at $\theta=0$ and π they are discarded. Further, the functions $P_n^m(\cos\theta)$ are taken to be defined as in

$$P_n^m(\cos\theta)=(-1)^m\sin^m\theta\frac{d^m P_n(\cos\theta)}{d(\cos\theta)^m} \tag{27}$$

where the Legendre polynomials $P_n(\cos\theta)$ are given by (Rodrigues' formula)

$$P_n(\cos\theta)=\frac{(-1)^n}{2^n n!}\frac{d^n\sin^{2n}\theta}{d(\cos\theta)^n} \tag{28}$$

An extensive discussion on the definition, recursion relations and orthogonality properties of the spherical harmonic functions and their applications to solve boundary-value problems in potential theory with special emphasis on electrostatics can be found in Refs. 17 and 18. The material in those two references or similar texts is absolutely indispensable to follow the present analysis and is not given here for the sake of brevity.

Zeroth-Order Potential, $U^{(0)}$

From Eqs. (20), (21), and (24) it is seen that,

$$\nabla^2 U^{(0)}=0 \text{ between } S_1 \text{ and } S_2 \tag{29}$$

$$U^{(0)}(a,\theta,\phi)=0 \quad (0\le\theta\le\theta;\ 0\le\phi\le 2\pi) \tag{30}$$

$$U^{(0)}(S_p)=1 \quad (S_p:\ r=b;\ 0\le\theta\le\theta^*;\ 0\le\phi\le 2\pi) \tag{31}$$

$$U^{(0)}(S_2-S_p)=0 \quad (r=b;\ \theta^*<\theta\le\pi;\ 0\le\phi\le 2\pi) \tag{32}$$

Solving by eigenfunction expansion,[18] it is easily seen that,

$$U^{(0)}(r,\theta,\phi)=\sum_{n=0}^{\infty}\frac{2n+1}{2}A_n R_n^{(0)}(r)P_n(\cos\theta) \tag{33}$$

where

$$R_n^{(0)}(r)=\frac{r^n-(a^{2n+1}/r^{n+1})}{b^n-(a^{2n+1}/b^{n+1})} \tag{34}$$

and

$$A_n=\int_0^{\theta^*}P_n(\cos\theta)\sin\theta\,d\theta=\int_\eta^1 P_n(\mu)\,d\mu, \qquad \eta=\cos\theta^* \tag{35}$$

First-Order Perturbation Potential, $U^{(1)}$

In addition to satisfying Laplace's equation in Eq. (20) and the homogeneous boundary condition equation (22) on the cavity wall, it is seen from Eq. (25) that,

$$U^{(1)}(a,\theta,\phi)=-\cos\gamma\frac{\partial U^{(0)}}{\partial r}(a,\theta,\phi) = \sum_{n=0}^{\infty}\frac{(2n+1)^2}{2a}\frac{\alpha^n}{\alpha^{2n+1}-1}A_n P_n(\cos\theta) \times\{\cos\theta\cos\theta_0+\sin\theta\sin\theta_0\cos\phi\} \tag{36}$$

where $\alpha=a/b$. Consistent with this boundary condition for ϕ dependence, a series solution for $U^{(1)}$ can be sought in the form,

$$U^{(1)}(r,\theta,\phi)=\sum_{m=0}^{1}\sum_{n=m}^{\infty}A_n^{(1)m}R_n^{(1)}(r)P_n^m(\cos\theta)\cos m\phi \tag{37}$$

where

$$R_n^{(1)}(r)=\frac{r^n-(b^{2n+1}/r^{n+1})}{a^n-(b^{2n+1})} \tag{38}$$

Substituting Eq. (37) into Eq. (36) and using the orthogonality properties of the spherical harmonics, it can be shown that,

$$A_n^{(1)0}=\cos\theta_0 D_n^{(1)0} \tag{39}$$

where

$$D_n^{(1)0}=\frac{(2n+1)(2n+3)}{2b}\frac{1}{\alpha^{n+3}-\alpha^{-n}}A_{n+1} + \frac{n(2n-1)}{2b}\frac{1}{\alpha^{n+1}-\alpha^{-(n-2)}}A_{n-1} \tag{40}$$

and

$$A_n^{(1)1}=\sin\theta_0 D_n^{(1)1} \tag{41}$$

where

$$D_n^{(1)1}=\frac{2n+3}{2b}\frac{1}{\alpha^{n+3}-\alpha^{-n}}A_{n+1} - \frac{(2n-1)}{2b}\frac{1}{\alpha^{n+1}-\alpha^{-(n-2)}}A_{n-1} \tag{42}$$

Second-Order Potential, $U^{(2)}$

Substituting the solutions for $U^{(0)}$ and $U^{(1)}$ in Eq. (26), the nonhomogeneous boundary condition for $U^{(2)}(a,\theta,\phi)$ is

seen to be of the form

$$U^{(2)}(a,\theta,\phi) = \sum_{m=0}^{2} f_m(\theta)\cos m\phi \tag{43}$$

Correspondingly, an eigenfunction expansion for $U^{(2)}$ is sought as in

$$U^{(2)}(r,\theta,\phi) = \sum_{m=0}^{2}\sum_{n=m}^{\infty} A_n^{(2)m} R_n^{(2)}(r) P_n^m(\cos\theta)\cos\phi \tag{44}$$

where $R_n^{(2)}(r) = R_n^{(1)}(r)$, given in Eq. (38).

From Eqs. (43) and (44) and the orthogonality of the spherical harmonics,

$$A_\ell^{(2)m} = \frac{2\ell+1}{2}\frac{(\ell-m)!}{(\ell+m)!}\int_0^\pi f_m(\theta) P_\ell^m(\cos\theta)\sin\theta\,d\theta \tag{45}$$

In particular,

$$A_n^{(2)0} = \cos^2\theta_0 E_n^{(2)0} + \sin^2\theta_0 F_n^{(2)0} \tag{46}$$

where

$$E_n^{(2)0} = \frac{1}{4b^2}\left\{\frac{n(n-1)(2n-3)}{\alpha^{n+1}-\alpha^{4-n}}\beta_{2n-1}A_{n-2} + \frac{2n+1}{\alpha^{n+3}-\alpha^{2-n}}\left[(n+1)^2\beta_{2n+3} + n^2\beta_{2n-1} - (2n+1)\right]A_n + \frac{(n+1)(n+2)(2n+5)}{\alpha^{n+5}-\alpha^{-n}}\beta_{2n+3}A_{n+2}\right\} \tag{47}$$

and

$$F_n^{(2)0} = \frac{1}{8b^2}\left\{\frac{n(n-1)(2n-3)}{\alpha^{4-n}-\alpha^{n+1}}\beta_{2n-1}A_{n-2} + \frac{2n+1}{\alpha^{n+3}-\alpha^{2-n}}\left[(n+1)^2\beta_{2n+3} + \frac{2(n+1)}{1-\alpha^{2n+3}} + n^2\beta_{2n-1} + \frac{2n}{1-\alpha^{1-2n}} - 3(2n+1)\right]A_n + \frac{(n+1)(n+2)(2n+5)}{\alpha^{-n}-\alpha^{n+5}}\beta_{2n+3}A_{n+2}\right\} \tag{48}$$

recalling, $\beta_k = (1+\alpha^k)/(1-\alpha^k)$.

Also,

$$A_n^{(2)1} = \sin\theta_0\cos\theta_0 D_n^{(2)1}$$

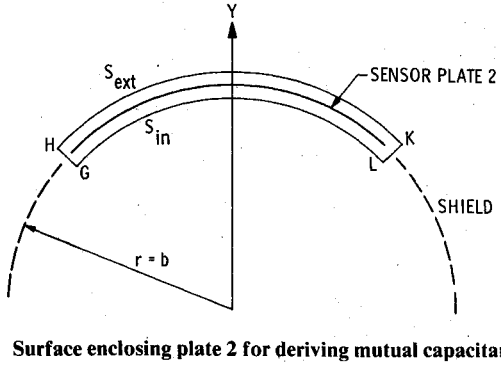

Fig. 3 Surface enclosing plate 2 for deriving mutual capacitance C_{12}.

where

$$D_n^{(2)1} = \frac{1}{2b^2}\left\{\frac{(n-1)(2n-3)}{\alpha^{4-n}-\alpha^{n+1}}\beta_{2n-1}A_{n-2} + \frac{2n+1}{\alpha^{2-n}-\alpha^{n+3}}\left[(1-\alpha^{2n+3})^{-1} + (\alpha^{1-2n}-1)^{-1}\right]A_n - \frac{(n+2)(2n+5)}{\alpha^{n+5}-\alpha^{-n}}\beta_{2n+3}A_{n+2}\right\} \tag{49}$$

$$A_n^{(2)2} = \sin^2\theta_0 D_n^{(2)2}$$

where

$$D_n^{(2)2} = \frac{1}{8b^2}\left\{\frac{(2n-3)}{\alpha^{n+1}-\alpha^{2-n}}\beta_{2n-1}A_{n-2} + \frac{2(2n+1)}{\alpha^{2-n}-\alpha^{n+3}}\left[(1-\alpha^{2n+3})^{-1} + (\alpha^{1-2n}-1)^{-1}\right]A_n - \frac{(2n+5)}{\alpha^{n+5}-\alpha^{-n}}\beta_{2n+3}A_{n+2}\right\} \tag{50}$$

Capacitance Coefficients

The spherical harmonic solutions for $U^{(0)}$, $U^{(1)}$, and $U^{(2)}$ can be substituted in Eq. (19) to obtain the potential distribution U corresponding to the case when sensor plate 1 is held at unit potential and all other conductors in the system are grounded. In turn, the potential U can be termwise differentiated and substituted in Eq. (11) and integrated over appropriate closed surfaces enclosing the individual conductors to obtain the capacitance coefficients C_{10} through C_{16} by Gauss' law.

Capacitance Coefficient C_{10}

The mutual-capacitance coefficient C_{10} (the induced charge on the proof-mass) is obtained from the surface integral.

$$C_{10} = -\epsilon_0\int_{S_0}\int \nabla U\cdot n\,ds \tag{51}$$

where S_0 is the surface of a sphere of radius $(a+d)$ centered at O and enclosing the proof-mass. Substituting for U in terms of the perturbation potentials,

$$C_{10} = -\epsilon_0(a+d)^2\int_{\theta=0}^{\pi}\int_{\phi=0}^{2\pi}\left\{\frac{\partial U^{(0)}}{\partial r} + d\frac{\partial U^{(1)}}{\partial r} + d^2\frac{\partial U^{(2)}}{\partial r}\right\}_{a+d}\sin\theta\,d\phi\,d\theta = (\epsilon_0 b)P\{1 + Ax + Bx^2 + D(y^2+z^2)\} \tag{52}$$

where

$$P = -2\pi\alpha/(1-\alpha) \tag{53}$$

$$A = 3(A_1/A_0)/(1-\alpha^3) \tag{54}$$

$$B = \frac{1}{1-\alpha^3}\left\{\frac{\alpha}{1-\alpha} + 5\frac{A_2}{A_0}\frac{1+\alpha^3}{1-\alpha^5}\right\} \tag{55}$$

and

$$D = \frac{\alpha}{1-\alpha^3}\left\{\frac{\alpha}{1-\alpha} - \frac{5}{2}\frac{A_2}{A_0}\frac{1+\alpha^3}{1-\alpha^5}\right\} \tag{56}$$

Also (x,y,z) are the coordinates of the center of the proof-mass in the Cartesian system, *but normalized* with respect to the cavity radius; in fact, from Fig. 1,

$$x=(d/b)\cos\theta_0$$

$$y=(d/b)\sin\theta_0\cos\phi_0$$

and

$$z=(d/b)\sin\theta_0\sin\phi_0 \tag{57}$$

Mutual Capacitance C_{12}

C_{12}, the mutual-capacitance coefficient, is the charge accumulated on sensor plate 2, when plate 1 only is at unit potential and is obtained from the surface integral,

$$C_{12}=-\epsilon_0\int_{S_{\text{in}}}\int \nabla U\cdot n\,ds \tag{58}$$

The nonzero contribution to the Gaussian charge integral arises only from the inner face S_{in} of the surface enclosing sensor plate 2, as shown in Fig. 3. Since plate 2 and the outer shield are at zero potential, ∇U is zero on the exterior face, S_{ext} in Fig. 3. For the same reason, ∇U is zero also on the lateral surface $GHKL$ except possibly at the circular edge GL, where, however, the surface area vanishes. Also, from Fig. 4, the limits of integration for the surface integral can be derived as

$$\theta_1=\left(\frac{\pi}{2}-\theta^*\right)\le\theta\le\left(\frac{\pi}{2}+\theta^*\right)=\theta_2$$

and

$$\phi_1=\phi_0-\cos^{-1}\left(\frac{\eta}{\cos\theta}\right)\le\phi\le\phi_0+\cos^{-1}\left(\frac{\eta}{\cos\theta}\right)=\phi_2 \tag{59}$$

Moreover, for the electrostatic force in Eq. (10) only the gradient ∇C_{ij} is necessary for $i,j\neq 0$. Hence the constant value of C_{12} (independent of proof-mass displacement d), obtained from

$$\frac{\partial U^{(0)}}{\partial r}(b,\theta,\phi)$$

is NOT explicitly evaluated. Then, it is seen that,

$$C_{12}=(\epsilon_0 b)\{E(x+y)+F(x^2+y^2)+Gz^2+Hxy\} \tag{60}$$

where

$$E=-\sum_{n=0}^{\infty} W_n D_n^{(1)0} I(0,n) \tag{61}$$

$$F=-\sum_{n=0}^{\infty} W_n E_n^{(2)0} I(0,n) \tag{62}$$

$$G=-\sum_{n=0}^{\infty} W_n F_n^{(2)0} I(0,n)+\sum_{n=2}^{\infty} W_n D_n^{(2)2} I(2,n) \tag{63}$$

$$H=-\sum_{n=1}^{\infty} W_n D_n^{(2)1} I(1,n) \tag{64}$$

$$W_n=(2n+1)\alpha^{n+1}/(1-\alpha^{2n+1}) \tag{65}$$

$$I(m,n)=\int_{\theta_1}^{\theta_2}\int_{\phi_1}^{\phi_2} P_n^m(\cos\theta)\cos m\phi\,\sin\theta\,d\phi\,d\theta \tag{66}$$

Self Capacitance C_{11}

The self capacitance of sensor plate 1 is obtained essentially following the steps for deriving C_{12}. However, the contribution to the capacitance integral from the corresponding exterior surface charge, far from being nonzero, could be very significant, since the plate is at unit potential and the outer shield is grounded. But the gap between the outer shield and the plate is much smaller than the gap between the plate and the proof-mass (at its closest approach to the cavity wall). Hence the contribution to C_{11} from the exterior surface charge can be considered independent of the proof-mass position and will NOT be explicitly evaluated.

The resulting expression for C_{11} (excluding terms independent of proof-mass displacement) is given by

$$C_{11}=(\epsilon_0 b)\{Kx+Lx^2+M(y^2+z^2)\} \tag{67}$$

where

$$K=-2\pi\sum_{n=0}^{\infty} W_n D_n^{(1)0} A_n \tag{68}$$

$$L=-2\pi\sum_{n=0}^{\infty} W_n E_n^{(2)0} A_n \tag{69}$$

and

$$M=-2\pi\sum_{n=0}^{\infty} W_n F_n^{(2)0} A_n \tag{70}$$

Capacitance C_{13}

From the physical considerations in deriving C_{12} and the algebraic manipulations for C_{11}, it is easily seen that,

$$C_{13}=(\epsilon_0 b)\{Ix^2+J(y^2+z^2)\} \tag{71}$$

where

$$I=2\pi\sum_{n=0}^{\infty} W_n E_n^{(2)0} T_n;\quad J=-2\pi\sum_{n=0}^{\infty} W_n F_n^{(2)0} T_n \tag{72}$$

and

$$T_n=\int_{\pi-\theta^*}^{\pi} P_n(\cos\theta)\sin\theta\,d\theta \tag{73}$$

Proof-Mass Self-Capacitance C_{00}

By definition, C_{00} is the ratio of the charge on the proof-mass to its potential when all the sensor plates and the shield are grounded. The potential distribution $U_B(r,\theta,\phi)$ corresponding to these boundary conditions can be obtained from $U(r,\theta,\phi)$ by letting $\theta^*=\pi$ and superposing a uniform potential of (-1) throughout the region bounded by S_1 and

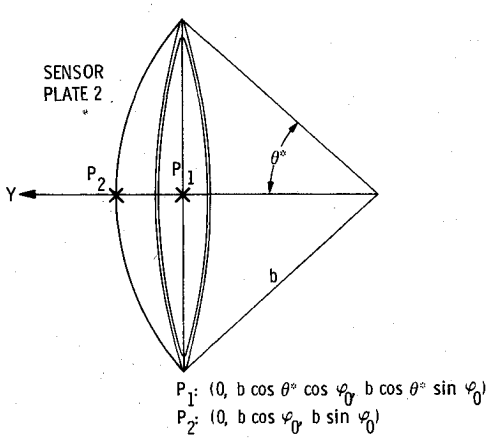

Fig. 4 Geometry of plate 2.

S_2. Denoting for convenience,

$$U_B(r,\theta,\phi) = -1 + U(r,\theta,\phi; \quad \theta^* = \pi) \tag{74}$$

it is easily seen that,

$$C_{00} = \epsilon_0 (a+d)^2 \int_{\theta=0}^{\pi} \int_{\phi=0}^{2\pi} \frac{\partial U_B}{\partial r} (a+d,\theta,\phi) \sin\theta \, d\phi \, d\theta$$

$$= (\epsilon_0 b) \frac{4\pi\alpha}{1-\alpha} \left\{ 1 + \frac{\alpha}{(1-\alpha)(1-\alpha^3)} (x^2+y^2+z^2) \right\} \tag{75}$$

When $d=0$, C_{00} reduces to the capacitance of a spherical condenser[19]; also, for $d>0$, the first nonzero correction term is proportional to d^2, calling for at least a second-order perturbation scheme as mentioned earlier.

Capacitance Matrix

From the algebraic expressions for C_{00}, and C_{10} through C_{13}, the entire capacitance matrix C_{ij} $(i,j=0, 1,\ldots,6)$ can be written out by simple coordinate transformations as in Ref. 20.

Results and Discussion

Capacitance Coefficients

The coefficients in the quadric expressions for self and mutual capacitance in Eqs. (52), (60), (67), and (71)—such as *P, A, B, D.*, ..., etc.—are dependent only on the ratio $\alpha = a/b$ and θ^*, the semivertical angle of the cone subtended by each sensor plate at the cavity center. From a computer program developed to evaluate these coefficients, the following results are obtained for a ratio of $\alpha = 0.55$ and $\theta^* = 35.5$ deg, the geometric parameters under consideration for a preliminary design:

$$C_{00} = (\epsilon_0 b) 15.36 \{ 1 + 1.46 (x^2+y^2+z^2) \} \tag{76}$$

$$C_{10} = -(\epsilon_0 b) 1.2 \{ 1 + 3.32x + 7.19x^2 - 1.4 (y^2+z^2) \} \tag{77}$$

$$C_{11} = (\epsilon_0 b) \{ 1.88x + 6.42x^2 - 0.77 (y^2+z^2) \} \tag{78}$$

$$C_{12} = (\epsilon_0 b) \{ 0.07 (x+y) - 0.77 (x^2+y^2) - 0.086z^2 - 0.06xy \} \tag{79}$$

$$C_{13} = (\epsilon_0 b) \{ 0.015x^2 - 0.27 (y^2+z^2) \} \times 10^{-2} \tag{80}$$

In addition to the data, $\alpha = 0.55$ and $\theta^* = 32.5$ deg, the following physical properties or constants also would be assumed for further reference: cavity radius, $b = 0.02$ m; and ball mass, $m_b = 0.2$ kg.

$$\epsilon_0 = 8.854 \times 10^{-12} \text{F/m}; \qquad g = 9.81 \text{ m/s}^2$$

SI units are used throughout further discussion.

The proof-mass self capacitance C_{00} can obviously be seen to be positive definite from Eq. (76). Substituting the values of ϵ_0 and b given above, C_{00} has a nominal value of 2.8 pF. Also, as the proof-mass is displaced directly toward a sensor plate by 50% of the gap, along the symmetry axis, the self capacitance C_{00} increases by about 7% of its nominal value. The mutual-capacitance coefficient C_{10} (between the proof-mass and sensor plate 1) is negative definite, since the ball is constrained to stay within the cavity, without touching its walls; actually, since (y^2+z^2) cannot exceed 0.2025, $C_{10} \leq -0.86\epsilon_0 b$. With the ball in the nominal position, the magnitude of the mutual capacitance $|C_{10}| = 0.2125$ pF; if the ball is moved toward sensor plate 1 with its center on the X axis by 50% of the gap, $|C_{10}|$ increases to 0.4463 pF. However, if the ball is displaced by the same amount, but with its center on the Y-Z plane, $|C_{10}|$ decreases to 0.1975 pF or a loss of about 7% of its nominal value.

It may be recalled that for $i, j \neq 0$, only terms corresponding to the *change in* C_{ij} due to ball displacement have been retained in the derivation. Accordingly, Eq. (78) shows the increase in the self capacitance C_{11} as the ball moves toward the plate in the $+X$ direction and also the decrease in C_{11} due to proof-mass motion in the (Y,Z) directions. Similarly, when the ball moves with its center in the X-Y plane, for positive values of x and y, the change in the mutual capacitance C_{12} is positive definite. In other words, as the ball moves towards plates 1 and 2, $|C_{12}|$ decreases due to electrostatic shielding.

Electrostatic Force

When the algebraic expressions for the capacitance coefficients such as in Eq. (52) are substituted in Eq. (10) and differentiated appropriately, the components of the electrostatic force can be derived as functions of the sensor plate potentials and the proof-mass charge and displacement. Proceeding further with numerical values, some sensitivity studies have been carried out in the current example, as described below.

Substituting the capacitance coefficients from Eqs. (76-80) in Eq. (10), the X component of the force is obtained:

$$F_X = (V_1 - V_3) \{ 0.769 (V_1 + V_3) - 0.209 V_T \} \times 10^{-11} + \{ K_1 x + K_2 y + K_3 z \} \times 10^{-11} - 0.026 (V_1 - V_3) (Q_0/b) + \{ 0.22 V_T - 1.35 (V_1 + V_3) \} (V_1 + V_3) \} (Q_0/b) x + 0.11 (Q_0/b)^2 x \times 10^{11} \tag{81}$$

where

$$K_1 = 0.35 V_T^2 + 5.59 (V_1^2 + V_3^2) - 0.68 \sum_{\ell=1}^{6} V_\ell^2 - 1.57 (V_1 + V_3) V_T + 2.12 V_1 V_3 - 0.0048 (V_2 V_4 + V_5 V_6) - 0.15 (V_2 + V_4) (V_5 + V_6) \tag{82}$$

$$K_2 = -0.97 (V_1 - V_3) (V_2 - V_4) \tag{83}$$

$$K_3 = -0.97 (V_1 - V_3) (V_5 - V_6) \tag{84}$$

and

$$V_T = V_1 + V_2 + V_3 + V_4 + V_5 + V_6 \tag{85}$$

From the general expression in Eq. (81) some specific problems can be examined to understand the system performance.

Charge-Acceleration Sensitivity

If the proof-mass carries a charge Q and is off-center, then even if all of the sensor plates are grounded, the resultant electrostatic force is given by

$$(F_X, F_Y; F_Z) = 2.7 \times 10^{13} Q^2 (x,y,z)$$

The charge required to produce an acceleration of $10^{-10} g$ of the proof-mass (0.2 kg) when it is off-center by 50% of the gap $(x = 0.225)$, works out to 5.7×10^{-12} C. In other words, a proof-mass charge in excess of 5×10^{-12} C would affect the system performance significantly.

Voltage Sensitivity

Space-charge effects are known[21] to contribute to a potential difference of several kilovolts between the different parts of a spacecraft. Although this does not seem likely[22] to happen in the Jovian or near-solar environment for the STARPROBE, it is still of interest to examine the instrument performance under differential potential because of the high sensitivity desired.

For instance, if sensor plate 1 were only to be raised to a potential of V_1 (volts), the proof-mass would experience a force,

$$F_X = \{5.6 + 36.9x\} V_1^2 \times 10^{-12}\text{N}$$

The voltage V_1 necessary to produce an acceleration of 10^{-10} g is simpy 6 V if the proof-mass were to be concentric with the cavity, and the same acceleration would result from a potential of $V_1 = 3.85$ V, if the ball were to be displaced toward sensor plate 1 by 50% of the gap. With the high sensitivity desired of the drag-free sensor, it is clearly seen that a differential potential of only a few volts could affect the system performance significantly.

Minimum Excitation Voltage

In practical systems, for onboard calibration, dithering, and for the design and implementation of charge estimation algorithms,[23] it is of interest to evaluate the minimum potential necessary to result in proof-mass motion of least measurable amplitude, say 1 μ or 10^{-6} m. Let the proof-mass carry a charge of 10^{-12} C and be concentric with the cavity. Suppose further that sensor plates 2, 4, 5, and 6 are grounded and alternating voltages are applied to sensor plates 1 and 3 such that,

$$V_1 = V\sin\omega t \quad \text{and} \quad V_3 = -V_1$$

The resulting force, $F_X = -26 \times 10^{-12}\ V\sin\omega t$, causes the proof-mass to oscillate at the same frequency, with $X(t) = X_0 \sin\omega t$. For an amplitude of $X_0 = 10^{-6}$ m, the minimum excitation potential, $V = V_{\min}$ is found to be 7.8 kV for $\omega = 1$ rad/s. Also it can be seen that $V_{\min}$ is directly proportional to ω^2.

Crosstalk Effects

It is also observed that if two *adjacent sensor plates only* (for instance, plates 1 and 2) are raised to some positive potential, then there is a resulting force in the X direction, even when the ball is displaced only in the Y direction and vice versa. (No charge on the ball is assumed in this discussion.) The X component of the force is given by

$$F_X = 0.33 \times 10^{-5} + 3.5 \times 10^{-5}x - 0.97 \times 10^{-5}y \qquad (86)$$

when

$$V_1 = V_2 = 1\text{ kV};\ V_3 = V_4 = V_5 = V_6 = 0 = Q$$

Or the magnitude of the acceleration in the X direction solely due to Y displacement is nearly 5×10^{-5} m/s^2 which is significant in view of the sensitivity of 10^{-11} m/s^2 expected of the sensor. Also, from the coefficients of the three terms in Eq. (86), the "cross-coupling term"—F_X resultant due to Y displacement of the proof-mass—is seen to be quite comparable in magnitude to the direct terms. When there is motion in the $+Y$ direction, there is change in the mutual capacitance coefficients between the proof-mass and the sensor plates on the Y axis. In particular, $|C_{20}|$ increases while $|C_{40}|$ decreases. Since $V_2 > 0$ and $V_4 = 0$, the stored energy in the system tends to increase. However, the force due to cross coupling tends to move the proof-mass in the $-X$ dirction, which, in turn, decreases $|C_{10}|$ and the stored energy as a counterbalancing measure. Similar effects also result from the mutual-capacitance coefficients C_{12} and C_{14}; however, their contribution is only 6% of the crosstalk effect, in the current example. These arguments are valid also for the forces in the Y and Z directions.

No "crosstalk" forces would be manifest if opposite plates are at the same potential.

Summary and Conclusions

A fully three-dimensional analysis of the electrostatics of a drag-free sensor for the STARPROBE has been carried out by a second-order boundary perturbation theory. The solutions for potentials and capacitance are obtained in terms of spherical harmonics and their integrals as appropriate. Simple quadric expressions for capacitance coefficients have been derived in terms of the proof-mass displacement and the sensor geometric parameters. The vector components of the electrostatic force also have been derived as quadric functions of the sensor place potentials and the proof-mass displacement and charge. The instrument sensitivity and functional capability have been examined for a typical design such as in the TRIAD satellite. However, it must be emphasized that improved methods of calculating the charge buildup, such as in Ref. 23, are essential for the accurate evaluation of proof-mass disturbances due to electrostatic forces.

Acknowledgments

This paper represents one phase of research performed by the Jet Propulsion Laboratory, California Institute of Technology, Pasadena, sponsored by the National Aeronautics and Space Administration, Contract NAS7-100.

References

[1] "STARPROBE Science Options Study and Final Report 1980-81—Advanced Technical Development Studies," JPL Publ. 715-127, Dec. 1981.

[2] Pisacane, V.L. et al., "Description of the Dedicated Gravitational Satellite Mission (GRAVSAT)," *IEEE Digest,* Vol. 1, 1981, pp. 254-269.

[3] "Combined GRAVSAT-TOPEX Study," Jet Propulsion Laboratory, Pasadena, Calif., Rept. 715-83, Aug. 15, 1980.

[4] Sonnabend, D., "Drag-free Is So Necessary," Jet Propulsion Laboratory, Pasadena, Calif., Interoffice Memo 312/79.7-137, Nov. 12, 1979.

[5] Sonnabend, D., "Study of a New Drag-Free Air Density Instrument Requiring No Propellant," Guidance and Control Laboratory, Dept. of Aeronautics and Astronautics, Stanford University, Stanford, Calif., April 1976.

[6] "A Satellite Freed of All But Gravitational Forces: TRIAD I," *Journal of Spacecraft and Rockets,* Vol. 11, Sept. 1974, pp. 637-644.

[7] Delattre, M., "L'accéléromètre ONERA a grande sensibilité," AGARD CP 43, May 1968.

[8] Bouttes, J., Delattre, M., and Juillerat, R., "Résultats des essais en vol de l'accéléromètre á haute sensibilité CACTUS," 21st IAF Congress, Constanz, Oct. 4-10, 1970.

[9] Exworthy, "Research in Electrically Supported Vacuum Gyroscope," Honeywell Inc., Rept. 20831-FR, (5 volumes), Nov. 1968.

[10] Smythe, W.R., *Static and Dynamic Electricity,* 3rd ed., McGraw Hill Book Co., New York, 1968, Sec. 2.20, pp. 39-40.

[11] Smythe, W.R., *Static and Dynamic Electricity,* 3rd ed., McGraw Hill Book Co., New York, 1968, Sec. 2.19, Eq. (2), p. 39.

[12] Smythe, W.R., *Static and Dynamic Electricity,* 3rd ed., McGraw Hill Book Co., New York, 1968, Sec. 2.16, Eq. (1), p. 37.

[13] Smythe, W.R., *Static and Dynamic Electricity,* 3rd ed., McGraw Hill Book Co., New York, 1968, Sec. 2.16, p. 37.

[14] Smythe, W.R., *Static and Dynamic Electricity,* 3rd ed., McGraw Hill Book Co., New York, 1968, Sec. 1.10, Eq. (1), p. 12.

[15]Smythe, W.R., *Static and Dynamic Electricity,* 3rd ed., McGraw Hill Book Co., New York, 1968, Sec. 3.02, Eq. (6), p. 50.

[16]Morse, P.M. and Feshback, H., *Methods of Theoretical Physics,* McGraw-Hill Book Co., New York, 1953, Chap. 9.

[17]Smythe, W.R., *Static and Dynamic Electricity,* 3rd ed., McGraw Hill Book Co., New York, 1968, Sec. 5.19, pp. 151-152. (Sections 5.12 through 5.44 discuss numerous applications of spherical harmonics and other special functions for problems in electrostatics.)

[18]MacRobert, T.M., *Spherical Harmonics,* 2nd revised ed., Dover Publications, New York, 1948.

[19]Smythe, W.R., *Static and Dynamic Electricity,* 3rd ed., McGraw Hill Book Co., New York, 1968, Sec. 2.03, Eq. (1), p. 27.

[20]"Electrostatic Analysis of a Drag-Free Sensor," Jet Propulsion Laboratory, Pasadena, Calif., Engineering Memo 347-128, Dec. 1981.

[21]Garrett, H.B., "Charging of Spacecraft Surfaces," *Reviews of Geophysics and Space Physics,* Vol. 19, Nov. 1981, pp. 577-616.

[22]Harel, M., "Charging of the Proof-Mass during the STAR-PROBE Mission," Jet Propulsion Laboratory, Pasadena, Calif., Engineering Memo 5137-81-148, Nov. 1981.

[23]Key, R.W., Mettler, E., Milman, M.H., and Schaechter, jD.B., "Spacecraft Drag-Free Technology Development," Jet Propulsion Laboratory, Pasadena, Calif., JPL Pub. 82-45, May 15, 1982.